ANTIOXIDANTS & REDOX SIGNALING
Volume 13, Number 1, 2010

DOI: 10.1089/ars.2009.2789

ORIGINAL RESEARCH COMMUNICATION

Impaired Liver Glucose Production in a Murine Model of Steatosis and Endotoxemia: Protection by Inducible Nitric Oxide Synthase

Oren Tirosh,[1] Avital Artan,[1] Michal Aharoni-Simon,[1] Giuliano Ramadori,[2] and Zecharia Madar[1]

Abstract

This study hypothesized that upregulation of inducible nitric oxide synthase (iNOS) would preserve the metabolic status of the liver under conditions of steatosis and acute inflammation. Wild-type C57BL/6J and C57BL/6 iNOS-knockout (-/-) mice were fed a choline-deficient ethionine-supplemented diet (CDE). Mice were also injected with 5 mg/kg lipopolysaccharide (LPS) to induce endotoxemia. Consumption of the CDE diet led to steatosis of the liver and decreased expression of the gluconeogenic genes compared wth controls. LPS treatment exacerbated these effects because of inhibition of *PGC-1α* expression, which resulted in hypoglycemia. In steatotic livers, LPS-induced iNOS expression was enhanced. Comparison between wild-type and iNOS-knockout mice under these conditions demonstrated a protective role of iNOS against fatal hypoglycemia. Nitric oxide (NO) signaling effects were confirmed by treatment of hepatocytes in culture with an NO donor, which resulted in increased expression of *PGC-1α* and gluconeogenic genes. In conclusion, iNOS was found to act as a protective protein and provides a possible mechanism by which the liver preserves glucose homeostasis under stress. *Antioxid. Redox Signal.* 13, 13–26.

Introduction

Along with an increasing prevalence of nonalcoholic fatty liver disease (NAFLD), a marked increase has occurred in individuals with metabolic impairments. One widespread imbalance is the insulin-resistance syndrome or metabolic syndrome, which refers to a constellation of symptoms, including glucose intolerance, obesity, dyslipidemia, and hypertension. This syndrome is known to promote the development of type 2 diabetes, cardiovascular disease, cancer, and other disorders. The liver plays a major role in the regulation of glucose, lipid, and energy metabolism, which are tightly regulated by insulin (18, 27). In addition, insulin resistance is now recognized as a pathologic factor in the development of NAFLD (18, 27). It has been suggested that prolonged elevation of the levels of sterol regulatory element–binding proteins (SREBPs) is responsible for the inhibition of insulin signaling in fatty liver (32). Hepatic insulin resistance can be defined as the failure of insulin to suppress hepatic glucose production adequately (38).

Several studies indicate the involvement of inflammatory activation in the development of hepatic and peripheral insulin resistance (1). Conversely, acute inflammation induced by lipopolysaccharides (LPSs) facilitates a hypoglycemic effect and impairment of hepatic glucose-6 phosphatase (*G6Pase*) expression (20, 21, 25). In critically ill patients, sepsis-induced hypoglycemia is a well-known event of unknown origin (35). The severity of sepsis is shown to correlate with the risk of sustaining hyperglycemia as well as critical hypoglycemia (16). Hypoglycemia during hospitalization occurs in patients with and without diabetes. In elderly hospitalized patients, a predicted increase in the in-hospital 3- and 6-month cumulative mortality has been documented (11). In addition, sepsis is 10 times more common in these patients than in nonhypoglycemic patients. Recently, it was shown that features of hepatitis and steatosis are the primary histologic findings in the liver of patients dying of sepsis (15). The hypoglycemic effect due to the fatty liver is also a known phenomenon in alcoholic patients and is related to the sudden death syndrome (4, 29, 41). Altogether, the accumulated data suggest that, although fatty liver and inflammation can generate a phenotype of insulin resistance, it can also lead to severe hypoglycemic life-threatening situations in patients with steatosis and

[1]The School of Nutritional Sciences, Institute of Biochemistry, Food Science and Nutrition, The Hebrew University of Jerusalem, Rehovot, Israel.
[2]Department of Internal Medicine, Section of Gastroenterology and Endocrinology, Georg-August-University, Göettingen, Germany.

acute inflammation due to an increase in hepatic insulin sensitivity (34, 35).

One of the main effects of the inflammatory response is the increased levels of inducible nitric oxide synthase (iNOS) in the liver. It was therefore postulated that nitric oxide (NO) would contribute to hepatotoxicity through the inhibition of ATP synthesis, increased reactive oxygen species (ROS), and the inability to adapt to hypoxic stress (22). Other studies imply that decreased production of NO from endothelial NOS contributes to liver pathology through dysregulation of blood flow and oxygen delivery (19). Furthermore, in iNOS-knockout mice, hepatocytes undergo necrosis and apoptosis after partial hepatectomy, indicating that the production of NO is essential to protect hepatocytes from death after liver resection (28).

The current study investigated the role of iNOS expression in mice subjected to a choline-deficient ethionine supplementation (CDE) diet that facilitates the development of fatty liver. Animals also were treated with LPS, which induces endotoxemia. The impact of these treatments on liver glucose–production pathways was determined.

Materials and Methods

Animals

Four- to five-week-old male C57BL/6J mice (Harlan Laboratories, Jerusalem, Israel) or C57BL/6J iNOS-knockout mice (Jackson Laboratories, Bar Harbor, ME) were treated with the CDE diet. The diet was choline deficient (MP Biomedicals, Irvine, CA) and supplemented with 0.15% ethionine in the drinking water (wt/vol; Sigma-Aldrich, St. Louis, MO) (3). Ethionine was used as an antagonist to methionine. The control group was fed the same diet + 0.2% choline chloride (wt/wt; Sigma-Aldrich) without the addition of ethionine to the drinking water. The mice were housed in plastic cages in a room maintained at 21°C to 22°C and illuminated in 12/12-h light–dark cycles. All animals received humane care, and all study protocols complied with the Hebrew University of Jerusalem's Animal Care Guidelines.

LPS treatment

After 14 days of feeding with CDE or control diets, food was removed for a 12-h overnight fast. Animals were then treated with a single IP injection of 5 mg/kg LPS (*Escherichia coli,* serotype 026:B6; Sigma-Aldrich, Rehovot, Israel). Control animals were injected with vehicle phosphate-buffered saline (PBS) (Invitrogen, Carlsbad, CA). Unless stated otherwise, animals were killed 6 h after the injections for tissue analysis.

Quantitative extraction of lipids from the livers

Lipids were extracted from liver tissue samples (100 mg). Extraction was performed by using 2 ml of Folch reagent made up of chloroform (J.T. Baker, Deventer, Netherlands) and methanol (Frutarom, Haifa, Israel), as previously described (8).

Blood liver enzymes and blood glucose evaluation

Glucose levels were determined in blood collected from mouse tail tips by using a hand-held glucometer (Medisense, Oxford, United Kingdom). For liver-enzyme evaluation, animals were anesthetized with Isoflurane (Minard. Inc., Bethlehem, PA), and blood samples were collected from the descending aorta into tubes containing heparin sodium (1 mg/ml, 20 μl). Hepatic cellular injury after the CDE diet and LPS treatments was determined with serum alanine aminotransferase (ALT, SGPT) and serum aspartate aminotransferase (AST, SGOT) levels. Analyses were performed by American Laboratories, Ltd. (Hertzlia, Israel).

Pyruvate tolerance test indicating liver glucose production

Liver glucose production was evaluated with a modified pyruvate tolerance test (PTT), carried out after overnight fasting. Initially, mice basal blood glucose levels were measured by using a glucometer (Medisense). Mice were then injected IP with 0.2 g per 1 kg body weight sodium pyruvate (Sigma-Aldrich, St. Louis, MO). One hour after the injection, blood glucose levels were measured as an indication of hepatic glucose production that resulted from the conversion of pyruvate to glucose through gluconeogenesis.

Evaluation of gene expression with real-time PCR

Total RNA extraction, reverse transcriptase (RT), and real-time PCR for detection of expression levels of iNOS, β-actin, peroxisome proliferator–activated receptor gamma coactivator-1α (*PGC-1α*), phosphoenol-pyruvate carboxykinase (*PEPCK*), and *G6pase* genes was performed. In brief, total RNA was prepared and isolated with the Tri-Reagent (Sigma-Aldrich, St. Louis, MO) method, according to the manufacturer's protocol. Total RNA (1 μg) was converted into cDNA by using the high-capacity cDNA Reverse Transcription kit (Applied Biosystems, Foster City, CA). Real-time PCR was performed by using the 7300 real-time PCR System (Applied Biosystems, Warrington, UK) and carried out with SYBR GREEN PCR Master Mix (Applied Biosystems). Sequences of oligonucleotides used as primers were as follows:

1. *PGC-1α*, left, 5′-AAACCCTGCCATTGTTAAG-3′, right, 5′-TGACAAATGCTCTTCGCTTT-3′
2. *PEPCK*, left, 5′-ACAGACTCGCCCTATGTGGT-3′, right, 5′-TGCAGGCACTTGATGAACTC-3′
3. *G6pase*, left, 5′-ACTCCAGCATGTACCGGAAG-3′, right, 5′-AAGAGATGCAGGAGGACCAA-3′
4. iNOS, left, 5′-AGCTCCCTCCTTCTCCTTCT-3′, right, 5′-TCTCTGCTCTCAGCTCCAAG-3′
5. eNOS, left, 5′-GAGCAGCACAAGAGCTACAAA-3′, right, 5′-GTGTTGCTAGACTCCTTCCTCTT-3′
6. β-Actin, left, 5′-CTAAGGCCAACCGTGAAAAG-3′, right, 5′-GGGGTGTTGAAGGTCTCAAA-3′.

The mixture was heated initially at 95°C for 10 min to activate hot-start DNA polymerase, followed by 40 cycles with denaturation at 95°C for 15 s and annealing at 60°C for 60 s. Each assay was performed simultaneously with samples and negative control (no RT samples), all in duplicate. Before the amplification, melt-curve protocols were performed to ensure that primer–dimers and other nonspecific products had been eliminated. DNA dilutions for the samples were set such that the ΔC_t between the target and the endogenous control genes was no more than five cycles.

Western blot analysis: iNOS, SREBP-1c and 4-hydroxynonenal-protein adducts level

Hepatic tissues (50 mg) were homogenized in lysis buffer containing 20 m*M* Tris, 145 m*M* NaCl, 10% glycerol, 5 m*M* EDTA, 1% Triton, 0.5% NP-40, and 0.2% protease inhibitor cocktail (Sigma-Aldrich, St. Louis, MO). Total protein was determined by using the Bradford reagent (Sigma-Aldrich, St. Louis, MO) with 2 mg/ml bovine serum albumin (Sigma-Aldrich, St. Louis, MO) as a standard. Samples (25 μg) were separated with 9% SDS-PAGE for iNOS or with 10% SDS-PAGE for SREBP-1c or for 4-hydroxynonenal (4HNE)-protein adducts by using a Bio-Rad (Hercules, CA) electrophoresis system, according to the manufacturer's instructions, and transferred electrophoretically to a nitrocellulose membrane (Whatman, Dassel, Germany). The transfer efficiency was evaluated with Ponceau S staining (Sigma-Aldrich, St. Louis, MO). Membranes were blocked in TBS (0.15 *M* NaCl, 10 m*M* Tris/HCl, pH 7.4) containing 5% (vol/vol) skimmed milk (BD Diagnostic Systems, Baltimore, MD)-Blotto, and then incubated overnight at room temperature with the primary antibodies for iNOS (rabbit anti iNOS; BD Biosciences, San Diego, CA) diluted 1:1,000 in TBST (TBS containing 0.05% vol/vol Tween 20), for SREBP-1c (rabbit anti SREBP-1c; Santa Cruz Biotechnology, Santa Cruz, CA) diluted 1:2,000 in TBST, for β-actin (mouse anti β-actin; BD Biosciences) diluted 1:2,500 in TBST and for 4HNE-protein adducts (mouse anti 4HNE; R&D Systems, Minneapolis, MN) diluted 1:1,000 in TBST. Next, the membranes were washed 4 times in TBST and incubated for 1 h with a secondary antibody (goat anti-rabbit; Jackson Immunoresearch, West Grove, PA) diluted 1:3,000 in 0.25% Blotto for the iNOS protein or diluted 1:4,000 in 2.5% Blotto for SREBP-1c, and with a secondary antibody (goat anti-mouse; Jackson Immunoresearch) diluted 1:2,500 in 2.5% Blotto for 4HNE-protein adducts or for β-actin. Membranes were exposed to Super ECL Western blotting detection reagents (Santa Cruz Biotechnology) and developed on film (Fuji Photo Film GmbH, Dusseldorf, Germany). Protein levels were evaluated with densitometry analysis by using Gel-pro Analyzer version 4.0 software (Media Cybernetics, Silver Spring, MD).

Liver histology

Hepatic steatosis and liver structural changes were assessed with histologic evaluation. Livers were fixed in 4% formaldehyde (Bio-Lab, Jerusalem, Israel), and microtome (Leica Microsystems, Wetzlar, Germany) sections (5 μm) were collected. Hematoxylin-eosin (H&E) (Sigma-Aldrich, St. Louis, MO) staining was used for tissue-section visualization.

AML-12 hepatocytes cell line treated with NO donor

Mouse hepatocyte AML-12 cells were grown in Dulbecco's Modified Eagle's Medium supplemented with 10% fetal calf serum, 1× glutamine, penicillin (100 U/ml), and streptomycin (100 mg/ml) at 37°C in a humidified atmosphere containing 95% air and 5% CO_2. Cells were exposed to 1 m*M* DETA-NONOate (Cayman Chemical, Ann Arbor, MI) diluted in 0.01 *M* NaOH for several time durations (12 to 36 h). Control cells were treated with 0.01 *M* NaOH (20). After the treatment, cells were washed with PBS (Invitrogen, Carlsbad, CA) and detached with 0.5 ml trypsin ×2 for total RNA isolation by the Tri-Reagent (Sigma-Aldrich, St. Louis, MO) method, according to the manufacturer's protocol and to real- time PCR as mentioned earlier with 18S as the reference gene. Primers 18S, left 5′- ACCGCAGCTAGGAATAATGG-3′, right 5′-CCTCAGTTCCGAAAACCAAC-3′.

Insulin determination

After relevant treatments, insulin measurements were performed in mouse serum collected after overnight fasting. For this, a two-site enzyme immunoassay with ultrasensitive mouse insulin ELISA (Mercodia AB, Uppsala, Sweden) was used, according to the manufacturer's instructions.

Statistical analysis

All values are expressed as means ± SEM. Comparisons between two groups were performed with Student's *t* test. For multiple groups, differences were considered significant at probability levels of $p < 0.05$ with the Tukey-Kramer HSD method. Statistical analysis was performed by using the statistical computer program, JUMP version 7 (SAS Institute, Cary, NC). Only significant differences are marked in the figures.

Results

Effect of CDE diet and LPS on liver gluconeogenesis

Effects of the CDE diet on the expression of key gluconeogenic enzymes was evaluated. Subjecting mice to 21 days of the diet led to a suppressed expression of hepatic *PEPCK* and *G6Pase* genes (Fig. 1A and B). Pathological evaluation of the CDE diet showed that steatosis that could be observed after 3 days reached 70 to 90% after 14 days. At 21 days, steatosis was decreased, and some fibrosis was observed. Therefore, all parameters were measured after 14 days on the CDE diet. Lipid content in the liver tissue was significantly elevated after only 7 days on the diet, and after 14 diet days, it reached a peak, as seen in Fig. 1D. Mice fed with the CDE diet for 14 days demonstrated lower body weight than did mice fed the control diet (Table 1). The CDE diet caused increased levels of liver aminotransferases ALT and AST in the blood (Fig. 1E and F). However, enzyme levels were lower than observed in mice treated with the CDE diet and LPS injection (Table 2, Exp. 2). Fasting blood glucose levels remained unchanged (Fig. 1C). To evaluate further the status of insulin sensitivity by following the CDE diet insulin serum levels, HOMA IR and expression of SREBP-1c were evaluated. Mice fed the CDE diet for 14 days had significantly lower plasma insulin levels and lower HOMA IR indices compared with controls, indicating greater insulin sensitivity (Fig. 2A and C). The CDE diet resulted in a significant decrease in the SREBP-1c protein level (mature form), as was evaluated with WB analysis (Fig. 2B). Levels of pre-SREBP-1c (125 kDa) were not detected in any of the mice.

Analysis of expression of the proinflammatory protein iNOS showed that giving a single injection of LPS to mice fed with the CDE diet for 14 days enhanced the expression of this protein compared with LPS treatment in control mice (Fig. 3A and B). In the absence of LPS, a CDE diet for 14 days did not induce expression of the iNOS protein (Fig. 3B). Consumption of the CDE diet for 14 days, LPS treatment, or a combination of both led to a decrease in eNOS mRNA levels compared

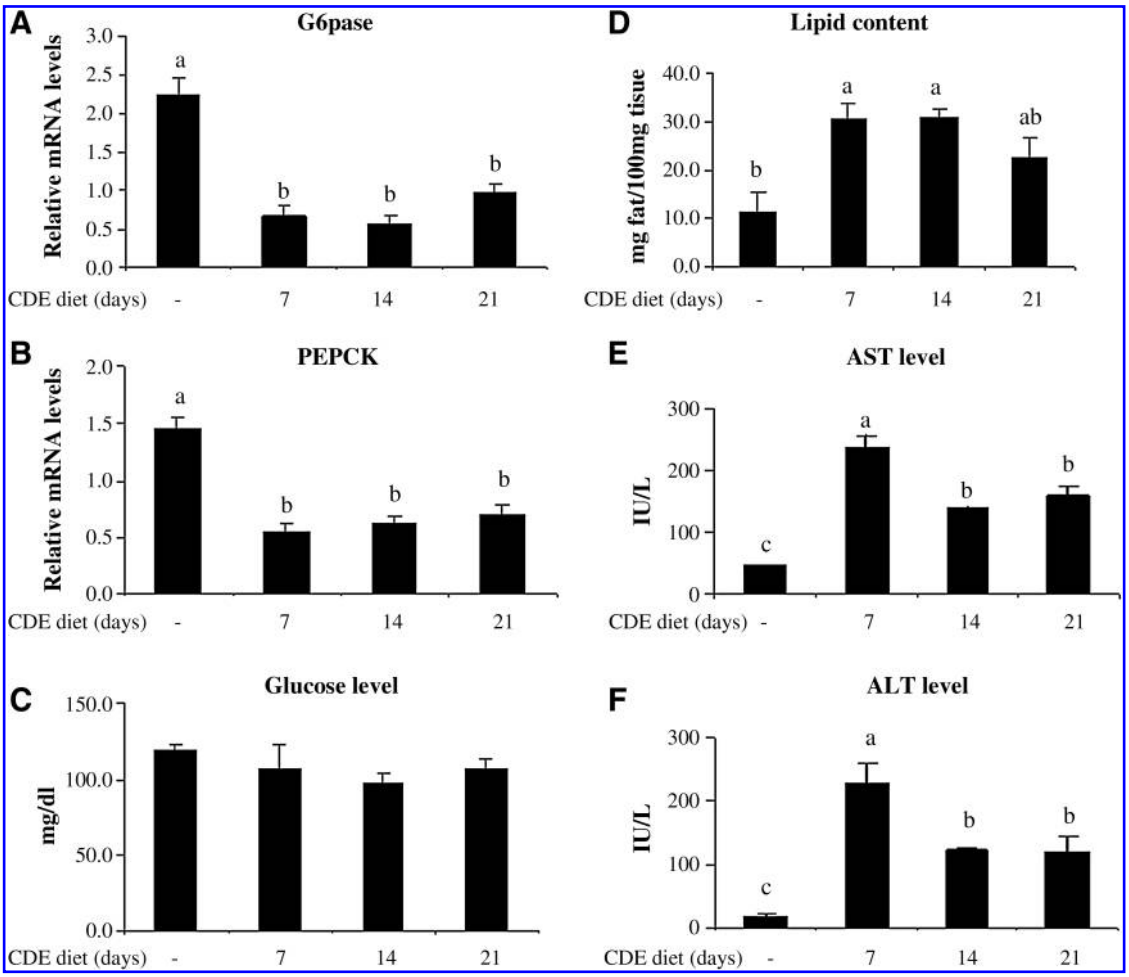

FIG. 1. Effect of the CDE diet on gluconeogenesis, liver lipid content, and blood levels of liver enzymes ALT and AST. Mice were treated with the CDE diet at several time points (7–21 days). Control group (-): mice fed a control diet for 21 days. (**A, B**) Expression of the gluconeogenesis key enzymes *G6pase* and *PEPCK* as evaluated with real-time PCR. Gene levels were normalized by using β-Actin as the reference gene. (**C**) Fasting blood glucose levels in mice serum. Values are expressed as mean $\pm$ SEM ($n = 8$ for each group). (**D**) Liver lipid extraction with the Folch reagent. (**E, F**) Blood levels of liver aminotransferases. Values are expressed as the mean $\pm$ SEM ($n = 5$ for each group). Means without a common letter are statistically different.

with those in control mice (Fig. 3D). Liver damage was not induced after 14 days on the CDE diet, although steatosis was observed in these animals (Fig. 3C).

The effect of different treatments on levels of steatosis was evaluated by quantitative extraction of lipids from the livers of the treated mice. The CDE diet was shown to facilitate lipid accumulation in the liver, whereas LPS injection had a negative effect on lipid levels in the liver (Table 1, Exp. 1).

Table 1. Effect of the CDE Diet on Average Weight in Mice

Treatment	*Average initial weight* $\pm$ *SEM*	*Average final weight* $\pm$ *SEM*
WT Control diet	18.2 ± 0.44	22.8 ± 0.44
WT CDE	18.4 ± 0.40	21.0 ± 0.44^a
iNOS(-/-) CDE	19.8 ± 0.82	20.0 ± 0.72^a

The 4- to 5-week-old mice were weighed at the beginning and at the end of the experiment (CDE diet for 14 days). WT and iNOS(-/-) mice treated with the CDE diet were compared with WT mice treated with control diet for 14 days.

[a] $p < 0.05$, significantly different from WT treated with control diet ($n = 5$).

To study the proinflammatory effect on glucose metabolism, the CDE diet was administered to mice for 14 days, followed by a single injection of LPS. Animals were killed 6 h after the LPS injection, and the effect on gluconeogenic gene expression was evaluated with real-time PCR. LPS dramatically decreased the expression of *PEPCK* and *G6Pase* in control animals and in CDE-treated animals (Fig. 4A and B), indicating that LPS injection suppressed glucose production by the liver (Fig. 4A and B), However, LPS led to a significant and more severe lowering of blood glucose levels after the CDE diet when compared with those in control animals (Fig. 4D).

To study potential mechanisms for this hypoglycemic effect, levels of *PGC-1α*, a co-activator that regulates the expression of key metabolic genes, including gluconeogenic genes, were evaluated. Interestingly, *PGC-1α* expression was upregulated in the CDE-treated animals (Fig. 4C).

Table 2. Total Lipid Content of the Liver after the Different Treatments and Levels of Liver Enzymes in the Blood

Treatment	*Liver lipid content (mg/100 mg tissue)*	*ALT (IU/L)*	*AST (IU/L)*
Exp.1 in WT mice			
Control	18.1 ± 0.7		
CDE	29.5 ± 4.9^a		
LPS	14.9 ± 0.8		
CDE+LPS	23.7 ± 3.6^a		
Exp. 2 in WT *vs*. iNOS(-/-) mice			
CDE+LPS: WT	24.8 ± 2.6	348.9 ± 44.4	405.3 ± 37.6
CDE+LPS: iNOS(-/-) mice	26.6 ± 4.5	749.9 ± 160.9^a	625.4 ± 117.2^a

Wild-type (WT) and iNOS-knockout mice were treated with CDE diet for 14 days followed by IP injection of LPS (5 mg/kg, 6 h).
ALT, alanine aminotransferase; AST, aspartate aminotransferase.
[a]$p < 0.05$.

However, this increase in *PGC-1α* expression did not lead to upregulation of expression of gluconeogenic enzymes (Fig. 4A and B) and was probably a response to counteract liver insulin sensitivity. After LPS injection, *PGC-1α* expression was significantly inhibited in CDE-treated mice (Fig. 4C).

iNOS expression protects the liver and preserves glucose homeostasis

It can be assumed that iNOS plays a key role in the development of liver damage. Alternatively, iNOS protein expression may serve as an adaptive response of the liver to

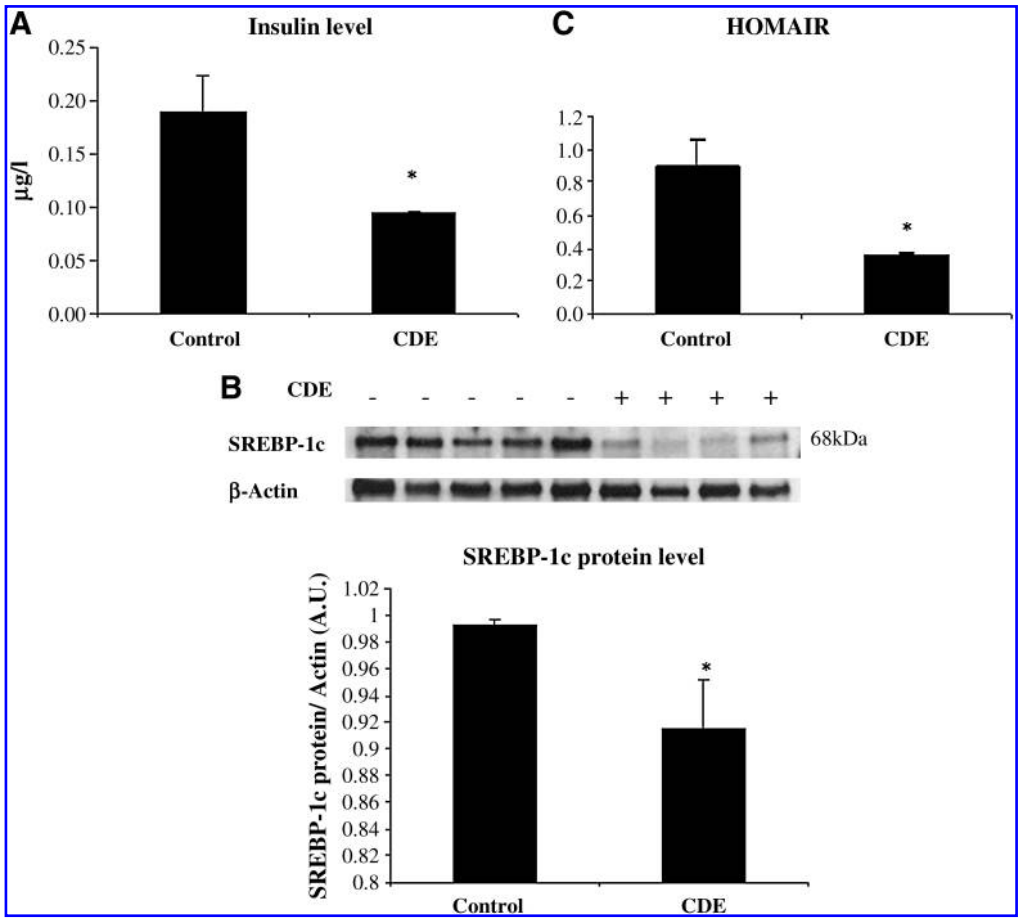

FIG. 2. Effect of the CDE diet on serum insulin levels, insulin sensitivity, and liver SREBP-1c. Mice fed the CDE diet for 14 days were compared with control mice. (**A**) Plasma insulin levels. Values are expressed as mean ± SEM ($n = 5$ different animal in each group). *$p < 0.05$. (**B**) SREBP-1c protein levels evaluated with the Western blot technique. Analysis by densitometry was performed ($n = 4$ for the CDE group, $n = 5$ for the control group) *$p < 0.05$. (**C**) HOMA IR evaluation: [Fasting blood glucose (mg/dl)×Insulin level (μU/ml)]/405). Values are expressed as mean ± SEM ($n = 5$ different animals in each group). *$p < 0.05$.

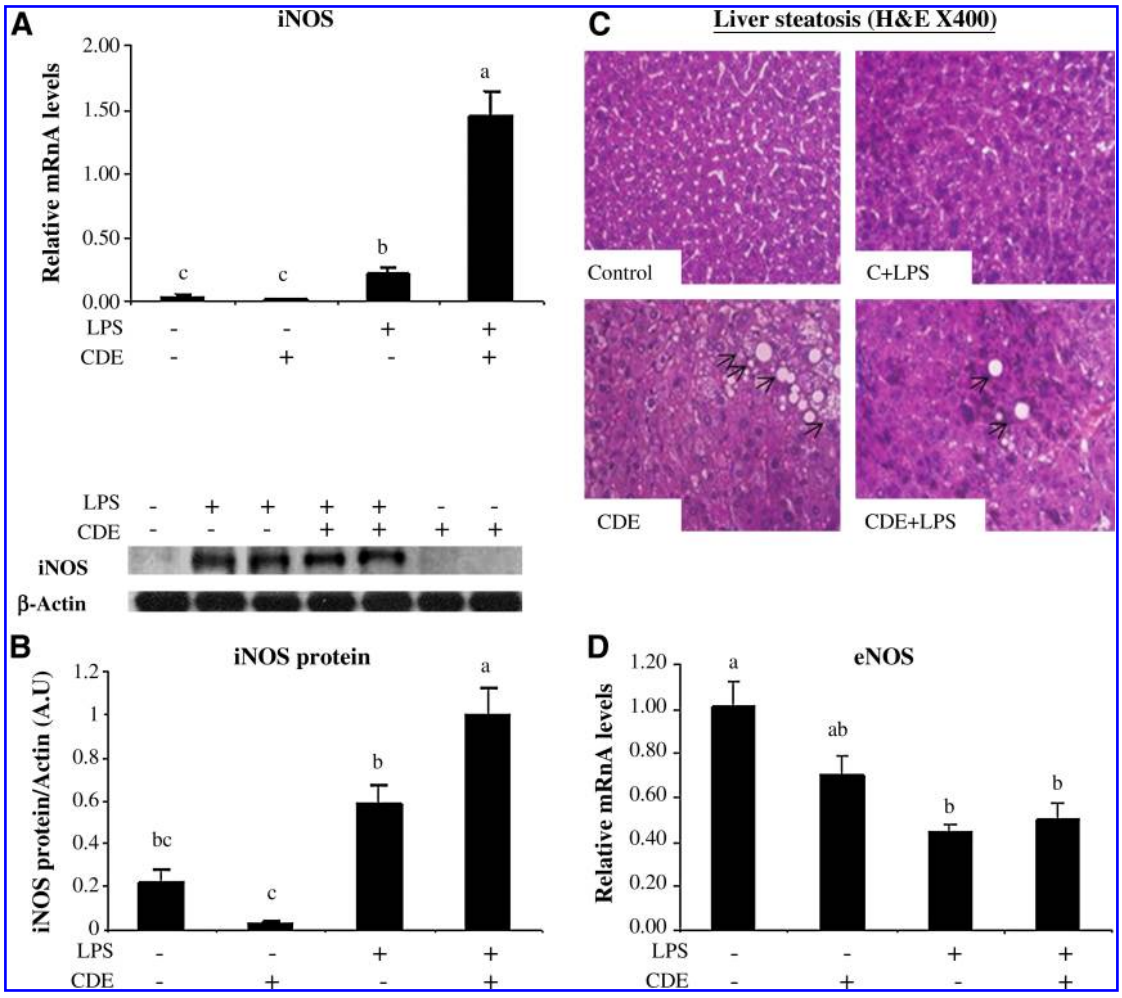

FIG. 3. Effect of LPS with and without the CDE diet on iNOS and eNOS expression and liver histology. (**A**) iNOS mRNA levels evaluated with real-time PCR (gene levels were normalized by using β-Actin as the reference gene). Values are expressed as the mean ± SEM ($n = 5$ for each group). (**B**) iNOS protein levels evaluated with Western blot technique after the CDE diet and LPS. Analysis by densitometry was performed ($n = 4$). Means without a common letter are statistically different ($p < 0.05$). (**C**) Representative liver histologic sections (5 μm) stained with H&E (magnification: ×400). *Arrows*, micro- and macrovesicular steatosis. (**D**) eNOS mRNA levels evaluated with real-time PCR (gene levels were normalized by using β-Actin as the reference gene). Values are expressed as mean ± SEM ($n = 5$ for each group). Means without a common letter are statistically different ($p < 0.05$). (For interpretation of the references to color in this figure legend, the reader is referred to the web version of this article at www.liebertonline.com/ars).

ameliorate such damage. To test this, iNOS-knockout animals were used. Figure 5A shows that after LPS injection in the iNOS (-/-) mice, hepatic iNOS protein was not expressed. In contrast, control wild-type (WT) littermates had easily identifiable levels of iNOS protein. Subjecting the iNOS (-/-) animals to the CDE diet, followed by LPS injection, revealed that animals lacking iNOS had significantly lower levels of gluconeogenic gene expression compared with WT animals (Fig. 5B–D). Of even greater importance was the finding that animals fed the CDE diet and treated with LPS were unable to maintain their normal blood glucose levels, which decreased to life-threatening levels 6 h after injection (Fig. 5E). The hypoglycemic effect of LPS + CDE in iNOS(-/-) could have resulted from increased insulin levels. However, this hypothesis was excluded after measurements of plasma insulin levels. In animals treated with CDE+LPS, insulin levels were higher in WT mice compared with iNOS (-/-) mice (Fig. 5F). These data demonstrate a critical role for iNOS protein in preserving the liver capacity to produce glucose by gluconeogenesis under conditions of stress.

Additionally, iNOS protein was demonstrated to prevent liver damage induced by the CDE diet and LPS injections, as shown by analysis of blood levels of the aminotransferases ALT and AST (Table 1, Exp. 2). Levels of liver enzymes in the blood were much higher in the iNOS(-/-) animals, whereas no difference in steatosis levels was found between the two animal types (Table 1, Exp. 2). Histologic H&E staining of liver sections supports these findings, and a higher level of damage was observed in livers of iNOS(-/-) mice (Fig. 6). Lipid peroxidation levels were evaluated with Western blot and densitometry analysis of 4-hydroxynonenal-protein adduct levels. Higher levels of lipid peroxidation were found in the livers of iNOS(-/-) mice treated with the CDE diet and LPS (Fig. 5G), compared with WT mice. Therefore, iNOS expression may act as a protective protein in fatty livers that are subjected to acute inflammation.

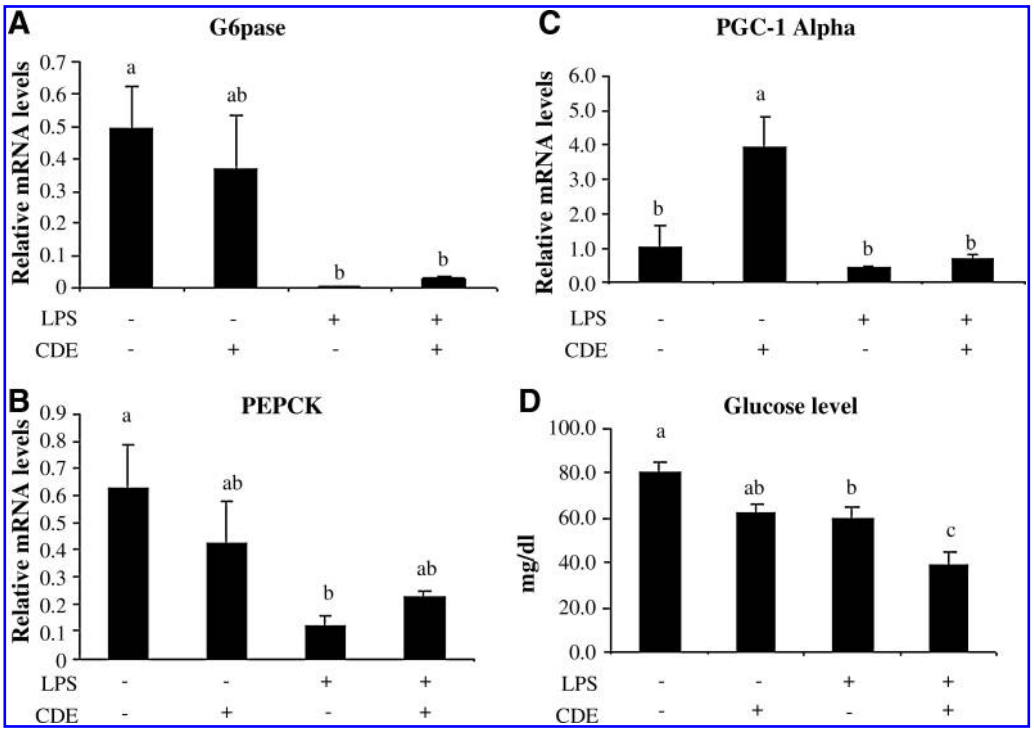

FIG. 4. Effect of LPS and the CDE diet on liver gluconeogenesis. mRNA levels showed changes in expression of the gluconeogenesis key enzymes, as evaluated with real-time PCR (gene levels were normalized by using β-Actin as the reference gene) (**A, B**), *G6pase*, and *PEPCK*. (**C**) Gluconeogenesis co-activator *PGC-1α*. (**D**) Fasting blood glucose levels in mice fed the CDE diet for 14 days and then treated with LPS (5 mg/kg) for 6 h. Values are expressed as the mean ± SEM ($n = 5$ for each group); Means without a common letter are statistically different ($p < 0.05$).

Blood glucose levels related to the kinetics of iNOS protein expression

Analysis of blood glucose levels of the iNOS(-/-) animals compared with control animals after CDE and LPS treatment showed that iNOS(-/-) animals had a lower capacity to maintain blood glucose levels (Fig. 7A). LPS initially induced an increase in blood glucose levels for the first 90 min after injection, and then blood glucose levels started to decline. iNOS(-/-) mice initially had lower blood glucose levels when compared with WT animals, but their capacity to elevate blood glucose levels after LPS injection was similar (Fig. 7A). In the iNOS(-/-) animals, severe hypoglycemia was observed 6 h after the LPS injection, from which they were unable to recover. Seven hours after LPS treatment, four of the knockout mice died of hypoglycemia, and the remainder were killed. No deaths occurred in the control WT group. In the control animals, blood glucose levels did not decrease below 50 mg/dl, and animals recovered from the inflammatory stress (Fig. 7A).

In control animals subjected to the CDE diet, iNOS expression was dominant in the hypoglycemic phase after the LPS injection. iNOS was not expressed during the initial hyperglycemic phase of up to 90 min after LPS injection (Fig. 7A and B).

Pyruvate tolerance test in WT mice compared with iNOS(-/-) mice

CDE and control supplemented mice were injected first with LPS. For evaluation of liver glucose production capacity, mice were treated 5 h after the LPS injection with 0.2 g/kg sodium pyruvate administered IP. Blood glucose levels were measured before the pyruvate challenge and 1 h later. The difference between blood glucose levels before and after the pyruvate tolerance test (PTT) showed a lower conversion of pyruvate to glucose in CDE-treated mice compared with control treated mice. iNOS(-/-) mice fed the CDE diet and treated with LPS (Fig. 8) had a much lower capacity to convert pyruvate to glucose. This farther supports the hypothesis that NO is an essential signaling molecule necessary for activation of gluconeogenesis in these conditions.

NO donor induced the expression of gluconeogenesis genes in the AML-12 cell line

NO donor (DETA-NONOate) treatment in AML-12 hepatocytes at several time points (12 to 36 h) showed a trend for increased *PEPCK* expression over time (Fig. 9A). Significant increases in *G6pase* expression levels were observed after 36 h (Fig. 9B). For *PGC-1α*, increased expression was observed after only 12 h of NO treatment (Fig. 9C). The temporal order of events indicated that NO can directly activate gluconeogenesis through upregulation of *PGC-1α* expression.

LPS-induced hypoglycemia in iNOS(-/-) mice fed control diet

Control and iNOS(-/-) animals not fed the CDE diet demonstrated equal sensitivity to LPS treatments. LPS treatment, as expected, decreased the expression of gluconeogenic genes and *PGC-1α* (Fig. 10A and B). Blood glucose levels decreased

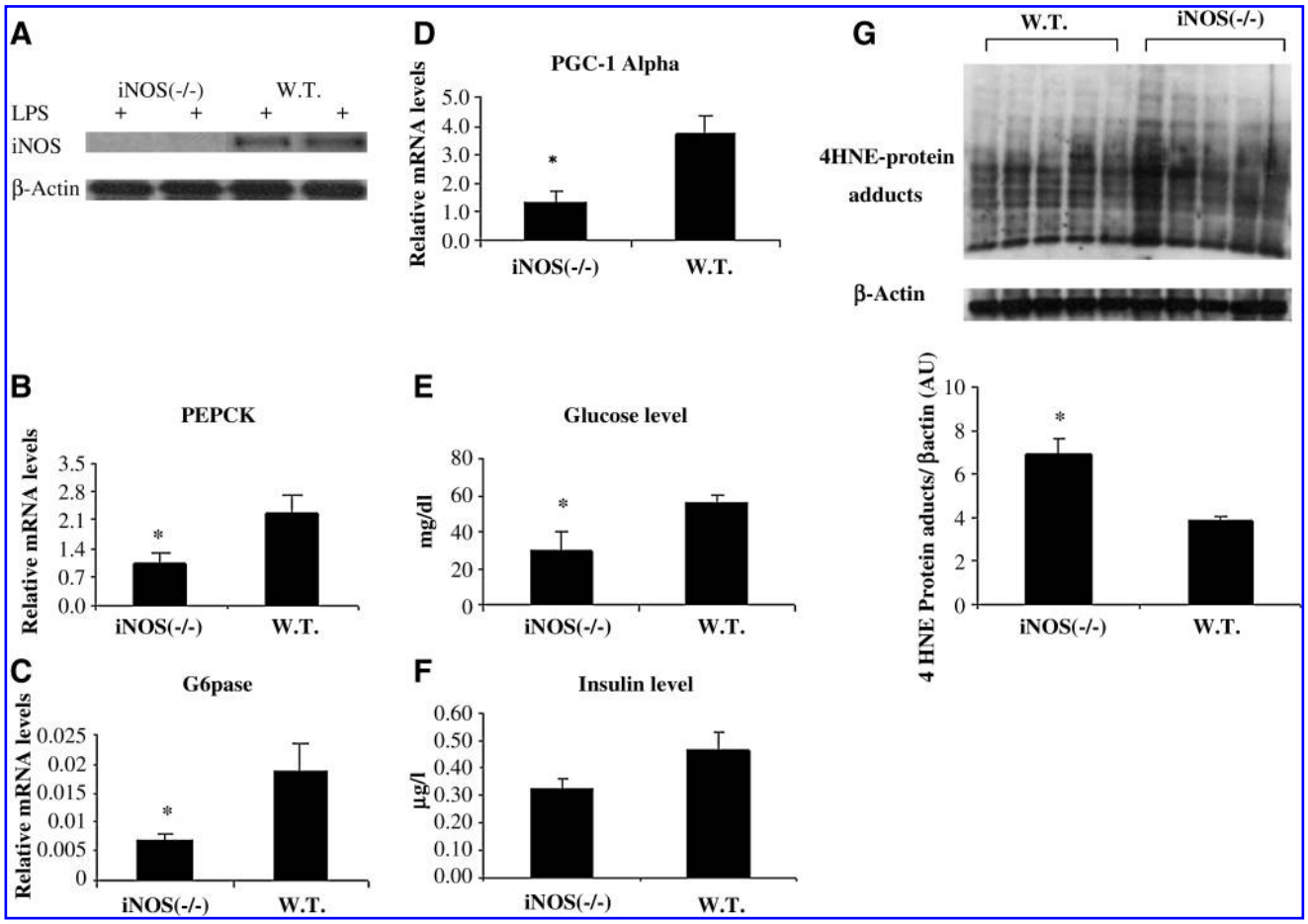

FIG. 5. Effect of the CDE diet and LPS injection on gluconeogenesis, insulin levels, liver damage, and lipid peroxidation in wild-type (WT) *vs*. iNOS-knockout mice. (**A**) To confirm knockout of the iNOS gene, protein levels were evaluated with the Western blot technique in WT mice (C57BL/6J) and iNOS-knockout mice, 6 h after IP injection of LPS (5 mg/kg). (**B–D**) WT mice and iNOS-knockout mice were treated with the CDE diet followed by LPS injection. *PEPCK*, *G6pase*, and *PGC-1α* expression were evaluated with real-time PCR (gene levels were normalized by using *β*-Actin as the reference gene). (**E**) Fasting blood glucose levels in iNOS-knockout mice *vs*. the WT mice after treatment with the CDE diet for 14 days and LPS (5 mg/kg) for 6 h. Values are expressed as mean ± SEM ($n = 9$ for each group). *$p < 0.05$. (**F**) Insulin-level evaluation in WT *vs*. iNOS(-/-) mice after the treatments. Values are expressed as mean ± SEM ($n = 5$ for each group). (**G**) Lipid peroxidation levels evaluated with Western blot of 4-hydroxynonenal-protein adduct levels and quantitative densitometric analysis of 4-hydroxynonenal-protein adduct levels. Values are expressed as mean ± SEM ($n = 5$ for each group). *$p < 0.05$.

as expected after LPS treatment for 6 h to levels of 50 to 60 mg/dl (Fig. 10C).

Discussion

In this study, induction of steatosis and liver damage was performed by using a CDE diet. This model mimics the situation of fatty liver (3) and was characterized by a decrease in the expression of key gluconeogenic enzymes and a trend for reduced blood glucose levels. Such a model is most relevant to liver pathology on a background of hypomethylation [*e.g.*, folic acid or vitamin B_{12} deficiency (36)]. The CDE model uses ethionine as a metabolic antagonist of methionine, and like the nonalcoholic steatohepatitis (NASH) model of methionine- and choline-deficiency diet (MCD model), did not generate an effect of insulin resistance (5, 17, 36). In this regard, MCD and CDE diets may provide an inaccurate model of common human NASH. The CDE-treated mice had a phenotype of insulin sensitivity with decreased blood insulin levels. The CDE diet upregulated the expression of *PGC-1α*, a coactivator of gluconeogenesis genes (26), a likely compensatory mechanism for the increased insulin sensitivity (Fig. 11). Downregulation in SREBP-1c levels may act as a possible molecular mechanism for the increased insulin sensitivity after consumption of the CDE diet. Because MCD and CDE diets may facilitate a fatty liver by inhibition of secretion of VLDL (10) from the liver, it is most logical that such diets would inhibit liver SREBP-1c–dependent lipogenesis, thereby abrogating the inhibitory effect of SREBP-1c on insulin signaling (32).

After LPS injection, the effect on gluconeogenic enzymes and *PGC-1α* expression was more apparent. LPS completely inhibited the upregulation of *PGC-1α* expression. The combination of CDE+LPS treatment led to impairment of hepatic gluconeogenic enzyme expression and glucose production, causing hypoglycemia (Fig. 11). The inhibitory effect of LPS on *PGC-1α* in steatotic livers was demonstrated in the current

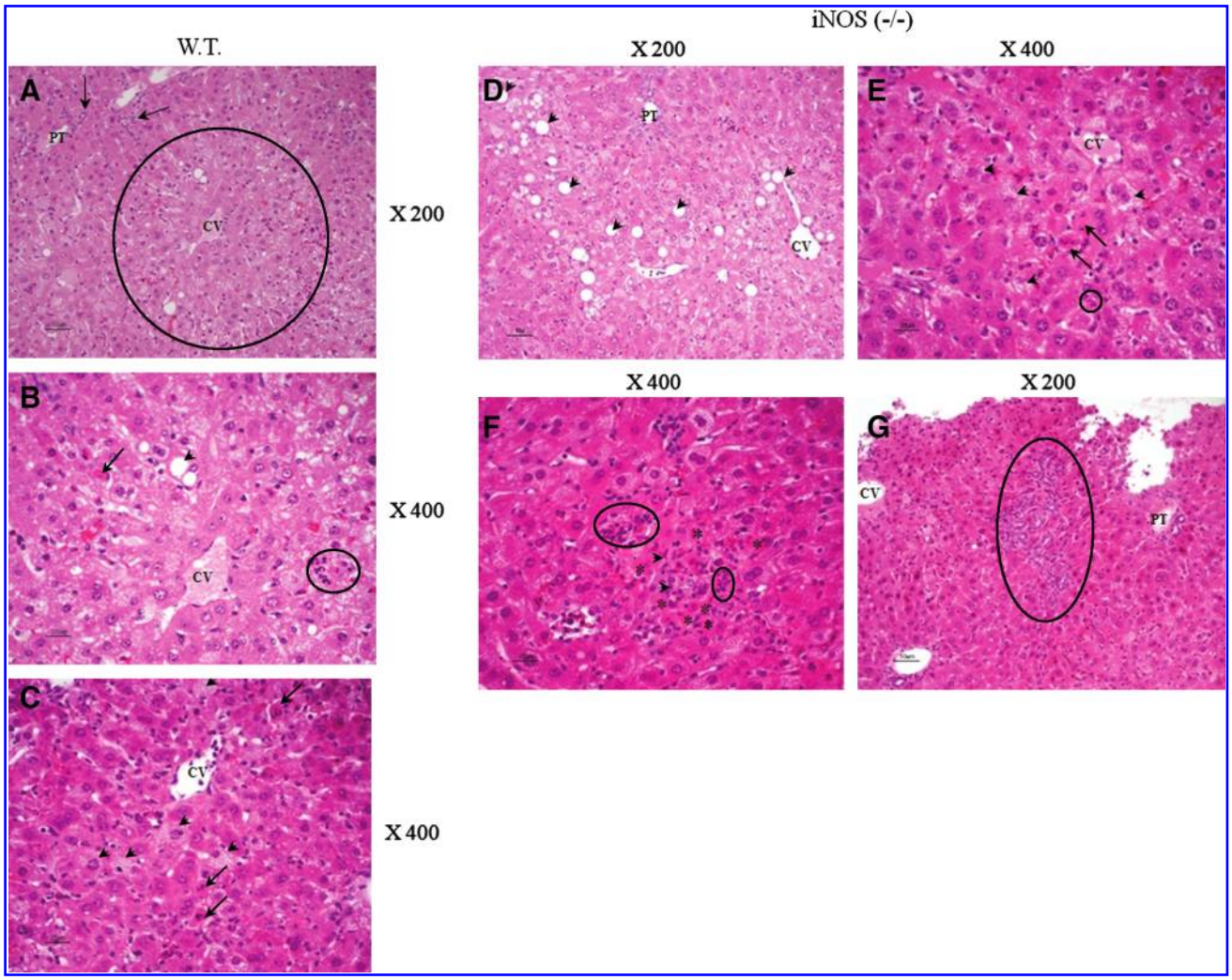

FIG. 6. Liver histologic sections demonstrating the effect of the CDE diet and LPS injection in iNOS(-/-) compared with WT mice. (**A**) Mild centrilobular hepatocellular vacuolation is evident. Most of the vacuoles are small (microvacuolation). Vacuolated hepatocytes are concentrated around the centrilobular venule (CV), within the circle. Hepatocytes near the portal triads (PT) have more-solid and darker-staining cytoplasm. *Arrows*, mild bile duct and oval cell hyperplasia arising from the portal triads. (**B**) High magnification. The vast majority of hepatocytes show microvacuolation, but a few contain larger cytoplasmic vacuoles, typical of lipid accumulation (*arrowhead*). An apoptotic hepatocyte is marked with an *arrow*. A small cluster of neutrophils is *circled*. (**C**) High magnification. Several apoptotic hepatocytes are identified with *arrows*. *Arrowheads*, hepatocytes with mild microvacuolation in iNOS(-/-) mice. (**D**) Moderate centrilobular hepatocellular vacuolation. Both microvacuoles and macrovacuoles (*arrowheads*) are present. The centrilobular venule (CV) and portal triad (PT) are identified. (**E**) *Arrows*, Apoptotic cellular debris. **Arrowheads**, Hepatocytes with mild cytoplasmic vacuolation. Clusters of neutrophils are *circled*. (**F**) High magnification showing a focus with accumulation of necrotic cellular debris (*asterisks*) mixed with neutrophils (*circled*) and a few mononuclear cells, consistent with Kupffer cells or macrophages (*arrowheads*). (**G**) This sample shows a focus of moderate bile duct and oval cell hyperplasia (circled). A ventrilocular venule (CV) and an unaffected portal triad (PT) are identified. (For interpretation of the references to color in this figure legend, the reader is referred to the web version of this article at www.liebertonline.com/ars).

study. Similarly, it has been shown in mice that LPS decreases fatty acid oxidation and nuclear hormone receptors in the kidney, diaphragm, heart, and liver during the acute-phase response induced by infection and inflammation. It also decreases the expression of *PGC-1α* and *β* coactivators (6, 7, 14).

Exposure of mice after the CDE diet to LPS resulted in increased liver damage compared with that in control animals. Indeed, genetically obese animals with fatty liver are known to be more sensitive to LPS-induced damage (39, 40). Evaluation of hepatic iNOS expression in these mice showed that after the LPS challenge, a higher expression of the protein was observed in fatty livers compared with normal livers. To evaluate whether iNOS expression and excessive NO production after the LPS challenge plays a protective role against inflammatory stress or promotes additional liver damage, similar treatments were performed in iNOS(-/-) mice. iNOS(-/-) mice were found to be more sensitive to damage induced by CDE+LPS. This effect was confirmed by the increased levels of blood liver enzymes. Therefore,

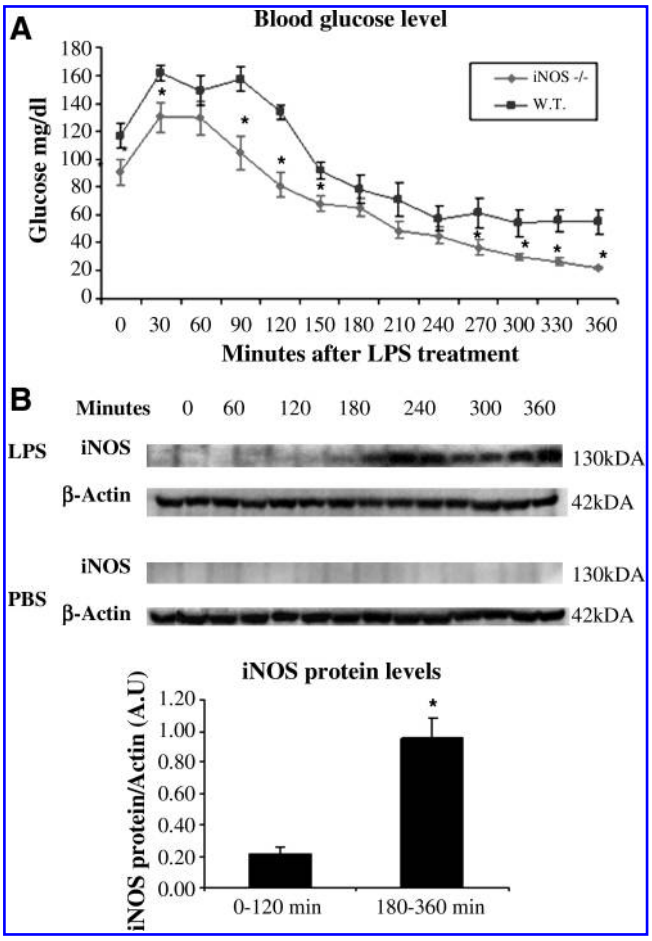

FIG. 7. Blood glucose levels and kinetics of iNOS protein expression. (**A**) Fasting blood glucose levels were measured in WT and iNOS-knockout mice treated with the CDE diet for 14 days at several time points (0–6 h) after LPS (5 mg/kg) treatment. Values are expressed as mean ± SEM ($n = 9$ for each group). *$p < 0.05$. (**B**) iNOS protein-level evaluation with the Western blot technique in WT mice with steatotic livers (CDE diet for 14 days). Several time points were evaluated (0 to 360 min) after treatment with LPS (5 mg/kg) or with PBS ($n = 2$). Densitometric analysis of iNOS expression and comparison between two time groups, 0–120 min and 180–360 min, is presented. The time points up to 120 min were compared with those from 180 min onward by a contrast t test within an ANOVA model comparing time points for repeated measures on the two samples; *$p < 0.05$.

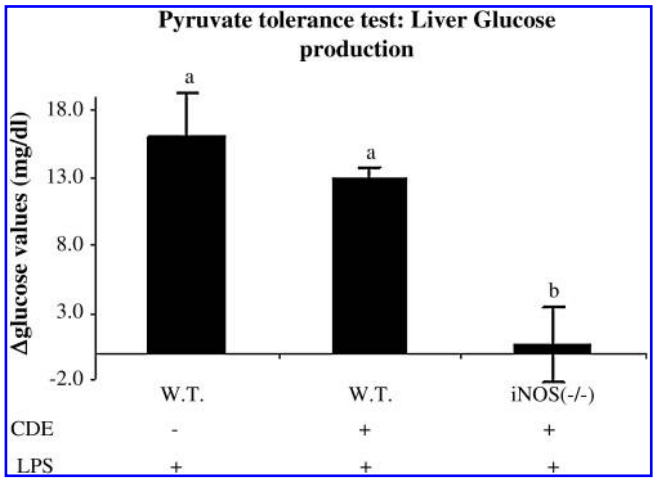

FIG. 8. Pyruvate tolerance test indicating glucose-production levels by the liver in iNOS(-/-) *vs.* WT mice fed the CDE or control diet and exposed to LPS treatment. WT mice treated with the CDE diet or with a control diet and iNOS(-/-) mice treated with the CDE diet for 14 days were injected with LPS (5 mg/kg). Five hours after the LPS treatment, all mice were injected with sodium pyruvate, 0.2 g/kg. Blood glucose levels were measured before the pyruvate injection and 1 h later. Glucose Δ values are presented as mean ± SEM ($n = 5$ for each group). Group means without a common letter are statistically different ($p < 0.05$).

upregulation of hepatic iNOS by inflammatory stimuli is a fast adaptive response to stress. iNOS also has a role in facilitating inflammatory reactions. However, in this study model, the protective effect of iNOS was evident. Interestingly, iNOS-derived nitric oxide generation actually protected the liver. One possible explanation could be that the levels of NO generated by the damaged liver were not in the toxic range because of substrate limitation. Therefore, iNOS-derived NO may function as an antioxidant (12, 13, 37) protecting against CDE or LPS capacity or both to induce liver damage. It has been demonstrated that injury to arginase-1–expressing cells, such as hepatocytes, leads to arginase-1 release into the circulation and increased arginase-1 plasma levels compromising arginine availability (2, 30) which may limit the NO production.

The effect of CDE and LPS to impair liver glucose–production systems was partially inhibited in the WT mice expressing iNOS compared with that in iNOS(-/-). Thus, it appears that CDE and LPS treatment in iNOS(-/-) mice facilitated severe liver damage, which resulted in a fatal hypoglycemic effect.

However, it also is possible that NO has a direct stimulatory effect promoting liver glucose production, making iNOS expression necessary for survival. This hypothesis that NO can directly activate gluconeogenesis (Fig. 9) was tested by using NO donors. Experiments performed with the NO donor DETA-NONOate in cultured hepatocytes showed a positive effect of NO on *PGC-1α* expression, and on the expression of gluconeogenic enzymes (Fig. 9). The temporal order of events after the NO treatment indicated that NO initially facilitated *PGC-1α* expression. Our data therefore indicate that NO generated by the iNOS protein can support the expression of *PGC-1α*. Nitric oxide produced by endothelial nitric oxide synthase was found to act as a signaling molecule that can activate the transcription factor co-activator *PGC-1α*, facilitating mitochondrial biogenesis (23, 24).

The hypoglycemic effect of LPS has been reported previously. Endotoxemia for 6 h resulted in a substantial increase in iNOS and COX-2 protein activity in lung and liver in correlation with liver and pancreatic dysfunction/injury, lactic acidosis, and hypoglycaemia. Prevention of LPS-induced hypotension and hypoglycemia by different pharmacologic agents was suggested to be partially mediated through inhibition of activities of the iNOS protein and cytokine formation. (20, 31). Here we show, for the first time, clear evidence

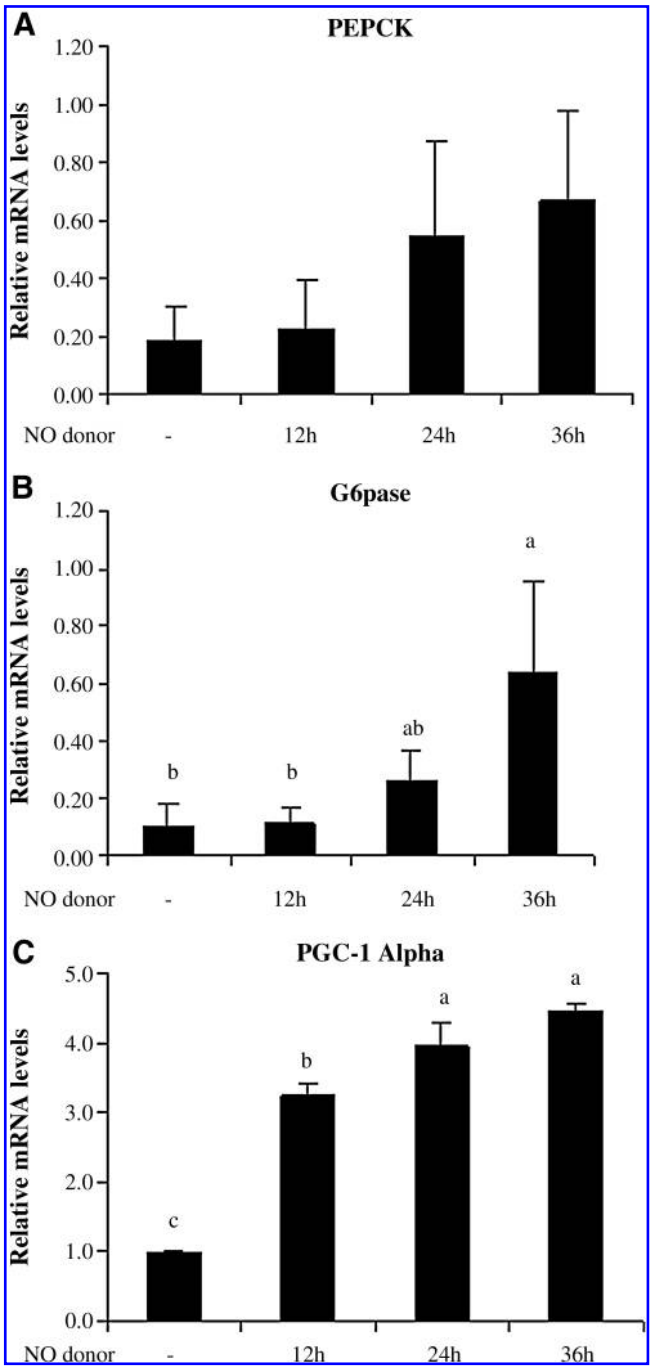

FIG. 9. Effect of a NO donor on *PEPCK*, *G6pase*, and *PGC-1α* expression in AML-12 hepatocytes. (**A–C**) NO donor (DETA-nonoate, 1 m*M*) increases *PEPCK*, *G6pase*, and *PGC-1α* expression at several time points (12–36 h) as evaluated with real-time PCR (gene levels were normalized by using 18S as the reference gene). Values are expressed as mean ± SD ($n = 3$). Group means with different letters are statistically different ($p < 0.05$).

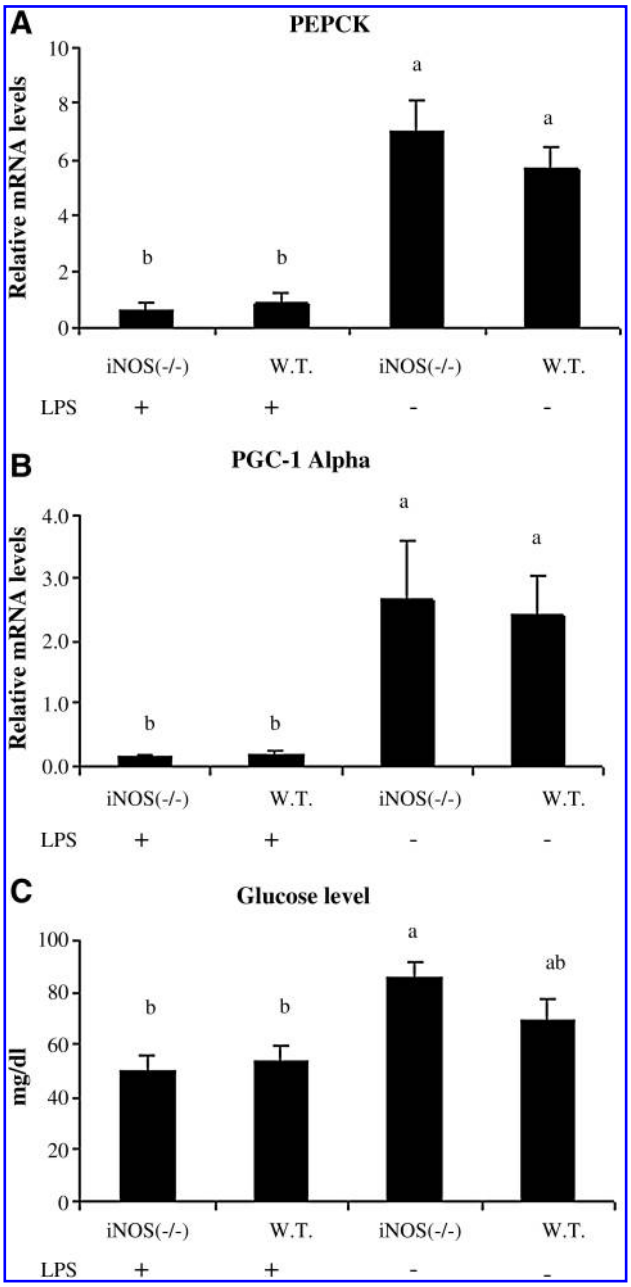

FIG. 10. Effect of LPS in iNOS(-/-) and WT mice fed control diets. (**A, B**) *PEPCK*, *PGC-1α* expression as evaluated with real-time PCR (gene levels were normalized by using *β*-Actin as the reference gene). (**C**) Fasting blood glucose levels in iNOS-knockout mice *vs*. WT mice after treatment with control diets for 14 days and with LPS (5 mg/kg) or with PBS for 6 h. Values are expressed as mean ± SEM ($n = 5$ for each group); means without a common letter are statistically different ($p < 0.05$).

that iNOS plays a role in counteracting the hypoglycemic effect of LPS rather than exacerbating it.

iNOS(-/-) mice were much more sensitive to CDE+LPS-induced severe hypoglycemia. The current study data, comparing the kinetic of expression of iNOS with blood glucose levels after an LPS injection, show that iNOS is not expressed during the initial hyperglycemic phase of LPS. iNOS is significantly expressed only during the later hypoglycemic phase. Moreover, iNOS(-/-) mice were unable to correct the detrimental hypoglycemia induced by LPS. Because of the biphasic effect of LPS to induce hyperglycemia followed by hypoglycemia, it was suggested that iNOS, as a major protein

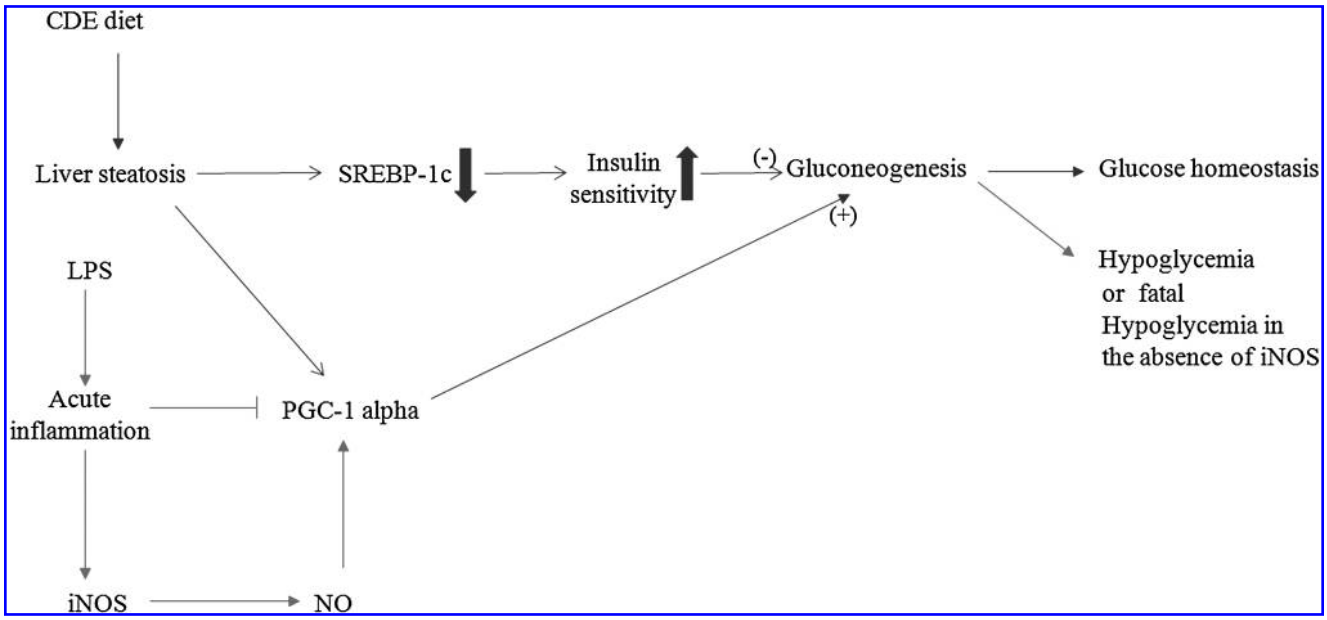

FIG. 11. Mechanism for fatty-liver–induced and LPS-induced hypoglycemia and protection by iNOS: Hypoglycemia occurs as a result of a combination of liver steatosis induced by the CDE diet that is accompanied by insulin sensitivity, and acute inflammation induced by LPS. SREBP-1c is lower in the CDE-treated mice than in mice fed a control diet. PGC 1α compensatory upregulation supports gluconeogenesis and preserves glucose homeostasis. Acute inflammation induced by LPS treatment reduces the expression of PGC 1α, the coactivator of gluconeogenesis, and leads to hypoglycemia. Acute inflammation in mice with fatty liver upregulates iNOS expression. NO production supports gluconeogenesis key enzymes through amplification of PGC 1α expression. In iNOS(-/-) mice with fatty liver, fatal hypoglycemia is observed after LPS treatment.

expressed in LPS-induced inflammation, is the link between inflammation and insulin resistance. Several studies indicate that iNOS is the cause of insulin resistance in fatty liver and obesity. Treatment with iNOS inhibitors reversed LPS-induced fasting hyperglycemia with concomitant amelioration of hyperinsulinemia and improved insulin sensitivity (9, 33). Yet, one of these studies showed only a small change in iNOS expression (9), and in another, no correlation between the kinetics of iNOS expression and the hyperglycemic effect of LPS was demonstrated (33). It should be noted that these studies were based on supplementation with iNOS inhibitors.

In conclusion, in a model of CDE diet followed by LPS injection, partial impairment of the capacity of the liver to produce glucose was observed. This was evident by the decreased expression of the rate-limiting gluconeogenic enzymes *PEPCK* and *G6Pase*. This effect was probably due to increased insulin sensitivity (Fig. 11). LPS further suppressed the liver gluconeogenic function. Based on levels of liver enzymes found in the blood, liver histology, and lipid peroxidation levels, NO produced by iNOS was found to be a protective signaling molecule to prevent liver damage after CDE+LPS treatment. In addition, iNOS helps to sustain liver glucose production under conditions of steatosis and acute inflammation.

This study demonstrated the first link between fatty liver, inflammation, and a hypoglycemic effect. The data shown could be highly relevant for patients with acute inflammation, treated in intensive care units, who also have high or marginal steatosis. Understanding the protective role of the iNOS protein against severe hypoglycemia due to hepatic insulin sensitivity may open the way for future treatments.

Acknowledgments

This study was supported a by grant 377/06 from the Israel Science Foundation to O.T. and Z.M. We thank Ms. Noga Budick-Harmelin for critical reading and reviewing.

Author Disclosure Statement

No competing financial interests exist.

References

1. Cai D, Yuan M, Frantz DF, Melendez PA, Hansen L, Lee J, and Shoelson SE. Local and systemic insulin resistance resulting from hepatic activation of IKK-beta and NF-kappaB. *Nat Med* 11: 183–190, 2005.
2. Cheng PN, Leung YC, Lo WH, Tsui SM, and Lam KC. Remission of hepatocellular carcinoma with arginine depletion induced by systemic release of endogenous hepatic arginase due to transhepatic arterial embolisation, augmented by high-dose insulin: arginase as a potential drug candidate for hepatocellular carcinoma. *Cancer Lett* 224: 67–80, 2005.
3. Davies RA, Knight B, Tian YW, Yeoh GC, and Olynyk JK. Hepatic oval cell response to the choline-deficient, ethionine supplemented model of murine liver injury is attenuated by the administration of a cyclo-oxygenase 2 inhibitor. *Carcinogenesis* 27: 1607–1616, 2006.
4. Denmark LN. The investigation of beta-hydroxybutyrate as a marker for sudden death due to hypoglycemia in alcoholics. *Forens Sci Int* 62: 225–232, 1993.
5. Fan JG and Qiao L. Commonly used animal models of nonalcoholic steatohepatitis. *Hepatobiliary Pancreat Dis Int* 8: 233–240, 2009.

6. Feingold KR, Moser A, Patsek SM, Shigenaga JK, and Grunfeld C. Infection decreases fatty acid oxidation and nuclear hormone receptors in the diaphragm. *J Lipid Res* 50: 2055–2063, 2009.
7. Feingold KR, Wang Y, Moser A, Shigenaga JK, and Grunfeld C. LPS decreases fatty acid oxidation and nuclear hormone receptors in the kidney. *J Lipid Res* 49: 2179–2187, 2008.
8. Folch J, Lees M, and Sloane Stanley GH. A simple method for the isolation and purification of total lipids from animal tissues. *J Biol Chem* 226: 497–509, 1957.
9. Fujimoto M, Shimizu N, Kunii K, Martyn JA, Ueki K, and Kaneki M. A role for iNOS in fasting hyperglycemia and impaired insulin signaling in the liver of obese diabetic mice. *Diabetes* 54: 1340–1348, 2005.
10. Jacobs RL, Lingrell S, Zhao Y, Francis GA, and Vance DE. Hepatic CTP:phosphocholine cytidylyltransferase-alpha is a critical predictor of plasma high density lipoprotein and very low density lipoprotein. *J Biol Chem* 283: 2147–2155, 2008.
11. Kagansky N, Levy S, Rimon E, Cojocaru L, Fridman A, Ozer Z, and Knobler H. Hypoglycemia as a predictor of mortality in hospitalized elderly patients. *Arch Intern Med* 163: 1825–1829, 2003.
12. Kanner J, Harel S, and Granit R. Nitric oxide as an antioxidant. *Arch Biochem Biophys* 289: 130–136, 1991.
13. Kanner J, Harel S, and Granit R. Nitric oxide, an inhibitor of lipid oxidation by lipoxygenase, cyclooxygenase and hemoglobin. *Lipids* 27: 46–49, 1992.
14. Kim MS, Shigenaga JK, Moser AH, Feingold KR, and Grunfeld C. Suppression of estrogen-related receptor alpha and medium-chain acyl-coenzyme A dehydrogenase in the acute-phase response. *J Lipid Res* 46: 2282–2288, 2005.
15. Koskinas J, Gomatos IP, Tiniakos DG, Memos N, Boutsikou M, Garatzioti A, Archimandritis A, and Betrosian A. Liver histology in ICU patients dying from sepsis: a clinico-pathological study. *World J Gastroenterol* 14: 1389–1393, 2008.
16. Krinsley JS. The severity of sepsis: yet another factor influencing glycemic control. *Crit Care* 12: 194, 2008.
17. Larter CZ and Yeh MM. Animal models of NASH: getting both pathology and metabolic context right. *J Gastroenterol Hepatol* 23: 1635–1648, 2008.
18. Leclercq IA, Da Silva Morais A, Schroyen B, Van Hul N, and Geerts A. Insulin resistance in hepatocytes and sinusoidal liver cells: mechanisms and consequences. *J Hepatol* 47: 142–156, 2007.
19. Liu J and Waalkes MP. Nitric oxide and chemically induced hepatotoxicity: beneficial effects of the liver-selective nitric oxide donor, V-PYRRO/NO. *Toxicology* 208: 289–297, 2005.
20. Lo YC, Wang CC, Shen KP, Wu BN, Yu KL, and Chen IJ. Urgosedin inhibits hypotension, hypoglycemia, and pro-inflammatory mediators induced by lipopolysaccharide. *J Cardiovasc Pharmacol* 44: 363–371, 2004.
21. Maitra SR, Gestring ML, El-Maghrabi MR, Lang CH, and Henry MC. Endotoxin-induced alterations in hepatic glucose-6-phosphatase activity and gene expression. *Mol Cell Biochem* 196: 79–83, 1999.
22. Mantena SK, King AL, Andringa KK, Eccleston HB, and Bailey SM. Mitochondrial dysfunction and oxidative stress in the pathogenesis of alcohol, and obesity-induced fatty liver diseases. *Free Radic Biol Med* 44: 1259–1272, 2008.
23. Nisoli E and Carruba MO. Nitric oxide and mitochondrial biogenesis. *J Cell Sci* 119: 2855–2862, 2006.
24. Nisoli E, Clementi E, Carruba MO, and Moncada S. Defective mitochondrial biogenesis: a hallmark of the high cardiovascular risk in the metabolic syndrome? *Circ Res* 100: 795–806, 2007.
25. Oguri S, Motegi K, Iwakura Y, and Endo Y. Primary role of interleukin-1 alpha and interleukin-1 beta in lipopolysaccharide-induced hypoglycemia in mice. *Clin Diagn Lab Immunol* 9: 1307–1312, 2002.
26. Puigserver P and Spiegelman BM. Peroxisome proliferator-activated receptor-gamma coactivator 1 alpha (PGC-1 alpha): transcriptional coactivator and metabolic regulator. *Endocr Rev* 24: 78–90, 2003.
27. Raddatz D and Ramadori G. Carbohydrate metabolism and the liver: actual aspects from physiology and disease. *Z Gastroenterol* 45: 51–62, 2007.
28. Rai RM, Lee FY, Rosen A, Yang SQ, Lin HZ, Koteish A, Liew FY, Zaragoza C, Lowenstein C, and Diehl AM. Impaired liver regeneration in inducible nitric oxide synthase deficient mice. *Proc Natl Acad Sci U S A* 95: 13829–13834, 1998.
29. Randall B. Fatty liver and sudden death: a review. *Hum Pathol* 11: 147–153, 1980.
30. Roth E, Steininger R, Winkler S, Langle F, Grunberger T, Fugger R, and Muhlbacher F. L-Arginine deficiency after liver transplantation as an effect of arginase efflux from the graft: influence on nitric oxide metabolism. *Transplantation* 57: 665–669, 1994.
31. Ruetten H and Thiemermann C. Effect of calpain inhibitor I, an inhibitor of the proteolysis of I kappa B, on the circulatory failure and multiple organ dysfunction caused by endotoxin in the rat. *Br J Pharmacol* 121: 695–704, 1997.
32. Shimano H. SREBP-1c and TFE3, energy transcription factors that regulate hepatic insulin signaling. *J Mol Med* 85: 437–444, 2007.
33. Sugita H, Kaneki M, Tokunaga E, Sugita M, Koike C, Yasuhara S, Tompkins RG, and Martyn JA. Inducible nitric oxide synthase plays a role in LPS-induced hyperglycemia and insulin resistance. *Am J Physiol Endocrinol Metab* 282: E386–E394, 2002.
34. Thompson BT. Glucose control in sepsis. *Clin Chest Med* 29: 713–720, x, 2008.
35. van der Crabben SN, Blumer RM, Stegenga ME, Ackermans MT, Endert E, Tanck MW, Serlie MJ, van der Poll T, and Sauerwein HP. Early endotoxemia increases peripheral and hepatic insulin sensitivity in healthy humans. *J Clin Endocrinol Metab* 94: 463–468, 2009.
36. Varela-Rey M, Embade N, Ariz U, Lu SC, Mato JM, and Martinez-Chantar ML. Non-alcoholic steatohepatitis and animal models: understanding the human disease. *Int J Biochem Cell Biol* 41: 969–976, 2009.
37. Volk J, Gorelik S, Granit R, Kohen R, and Kanner J. The dual function of nitrite under stomach conditions is modulated by reducing compounds. *Free Radic Biol Med* 47: 496–502, 2009.
38. Weickert MO and Pfeiffer AF. Signalling mechanisms linking hepatic glucose and lipid metabolism. *Diabetologia* 49: 1732–1741, 2006.
39. Yang S, Lin H, and Diehl AM. Fatty liver vulnerability to endotoxin-induced damage despite NF-kappaB induction and inhibited caspase 3 activation. *Am J Physiol Gastrointest Liver Physiol* 281: G382–G392, 2001.
40. Yang SQ, Lin HZ, Lane MD, Clemens M, and Diehl AM. Obesity increases sensitivity to endotoxin liver injury: implications for the pathogenesis of steatohepatitis. *Proc Natl Acad Sci U S A* 94: 2557–2562, 1997.
41. Yuzuriha T, Okudaira M, Tominaga I, Hori S, Suzuki H, Matsuo Y, Shoji M, Yokoyama A, Takagi S, and Hayashida

M. Alcohol-related sudden death with hepatic fatty metamorphosis: a comprehensive clinicopathological inquiry into its pathogenesis. *Alcohol Alcohol* 32: 745–752, 1997.

Address correspondence to:
Oren Tirosh
The School of Nutritional Sciences
Institute of Biochemistry, Food Science and Nutrition
The Hebrew University of Jerusalem
Rehovot
Israel

E-mail: otirosh@agri.huji.ac.il

Date of first submission to ARS Central, July 22, 2009; date of final revised submission, November 9, 2009; date of acceptance, December 1, 2009.

Abbreviations Used

4HNE = 4-hydroxynonenal
ALT = alanine aminotransferase
AST = aspartate aminotransferase
CDE = choline-deficient ethionine-supplemented diet
G6pase = glucose-6 phosphatase
H&E = hematoxylin and eosin
iNOS = inducible nitric oxide synthase
LPS = lipopolysaccharide
MCD = methionine and choline deficiency diet
NAFLD = nonalcoholic fatty liver disease
NASH = nonalcoholic steatohepatitis
NO = nitric oxide
PBS = phosphate-buffered saline
PEPCK = phosphoenol-pyruvate carboxy kinase
PGC-1α = peroxisome proliferator–activated receptor gamma coactivator-1α
PTT = pyruvate tolerance test
ROS = reactive oxygen species
RT = reverse transcriptase
SREBPs = sterol regulatory element–binding proteins
WT = wild type

This article has been cited by:

1. Michal Aharoni-Simon, Sarit Anavi, Uwe Beifuss, Zecharia Madar, Oren Tirosh. 2012. Nitric oxide, can it be only good? Increasing the antioxidant properties of nitric oxide in hepatocytes by YC-1 compound. *Nitric Oxide* **27**:4, 248-256. [CrossRef]
2. Eleni A. Karavia, Dionysios J. Papachristou, Ioanna Kotsikogianni, Irene-Eva Triantafyllidou, Kyriakos E. Kypreos. 2012. Lecithin/cholesterol acyltransferase modulates diet-induced hepatic deposition of triglycerides in mice. *The Journal of Nutritional Biochemistry* . [CrossRef]
3. Sabine Wagnerberger, Astrid Spruss, Giridhar Kanuri, Valentina Volynets, Carolin Stahl, Stephan C. Bischoff, Ina Bergheim. 2012. Toll-like receptors 1–9 are elevated in livers with fructose-induced hepatic steatosis. *British Journal of Nutrition* **107**:12, 1727-1738. [CrossRef]
4. Michal Aharoni-Simon, Michal Hann-Obercyger, Svetlana Pen, Zecharia Madar, Oren Tirosh. 2011. Fatty liver is associated with impaired activity of PPAR#-coactivator 1# (PGC1#) and mitochondrial biogenesis in mice. *Laboratory Investigation* **91**:7, 1018-1028. [CrossRef]
5. Yael Dinur Schejter, Elliot Turvall, Zvi Ackerman. 2010. Characteristics of Patients With Sulphonurea-Induced Hypoglycemia. *Journal of the American Medical Directors Association* . [CrossRef]